International Journal of Dynamics and Control (2023) 11:1132–1141
https://doi.org/10.1007/s40435-022-01033-0

Spacecraft reentry trajectory optimization by heuristic optimization methods and optimal control theory

Alireza Ekrami Kivaj[1] · Alireza Basohbat Novinzadeh[2] · Farshad Pazooki[1]

Received: 2 March 2022 / Revised: 18 July 2022 / Accepted: 28 August 2022 / Published online: 12 October 2022

Abstract

In the present work, a hybrid method for trajectory optimization of reentry spacecraft was proposed. The guiding legislation on the basis of heat reduction is presented in the procedure of obtaining the optimal trajectory. The heat rate should be decreased in the early phase of reentry flight by concentrating on the angle of attack profile. To meet terminal circumstances, the second step of suggested guidance included specifying the accurate profiles of the angle of attack and bank angle. A specific cost function should be minimized in each step. As a result, many optimization strategies have been utilized and compared. Due to its long flight duration and numerical sensitivity, the optimum trajectory issue of the space reentry vehicle (SRV) has been explored as one of the toughest problems in trajectory design. In both phases, the ideal trajectory for the optimality requirements has been discovered for various cost functions such as (i) overall heat rate, (ii) maximal heat rate, and (iii) terminal conditions. It may be inferred that the unique suggested strategy can minimize heat while maintaining the final conditions.

Keywords Optimal control · Trajectory optimization · Spacecraft reentry · Heuristic optimization · Dividing guidance method · Heat transfer rate

1 Introduction

It is inevitable to enter the atmosphere in order to recover important cargo from space. Under the pull of gravity, the vehicle travels at hypersonic speeds throughout its return journey. The car heats up as a result of the high speed. As a result, thermal shielding is necessary for spaceship safety. One of the most basic techniques to minimize heat is to design an appropriate return route.

Many problems in astronautics and aeronautics may be expressed as optimal control and trajectory optimization problems. The optimum control theory was well-known in the early 1960s as a result of the exceptional performance of optimal trajectory designs in aeronautical applications [1]. In reality, Lev Pontryagin and coworkers [2] addressed a variety of variations and expansions of the fundamental problems. Different types of numerical solutions for optimal control problems may be found. One of the essential methods for solving optimal control problems is to use an indirect approach based on the calculus of variations. The first-order optimality condition is used in this manner to solve the two-point boundary value problem in order to solve the optimal control problem. The direct technique, in which the control problem is discretized after parameterization, is the other option. As a consequence, the resultant finite-dimensional optimization problem is solved using the nonlinear programming approach. The numerical resilience of this strategy, which is dependent on the initial estimate, is well-known, as is its effectiveness in many difficult situations [3, 4]. In terms of heuristical optimizers, a separate category of direct techniques is global optimization. This strategy has lately piqued people's curiosity. The solution domain of the optimization problem is studied in the global optimization approach to locate all optimum solutions [5]. In this fashion, various

✉ Alireza Basohbat Novinzadeh
novinzadeh@kntu.ac.ir

Alireza Ekrami Kivaj
alireza.ekrami10@gmail.com

Farshad Pazooki
pazooki_fa@srbiau.ac.ir

1 Department of Aerospace Engineering, Science and Research Branch, Islamic Azad University, Tehran, Iran

2 Department of Aerospace Engineering K. N, Toosi University of Technology, Tehran, Iran

experiments on modified genetic algorithms (GA) for trajectory optimization have been conducted [6]. Particle swarm optimization (PSO) has also been employed for trajectory optimization in the reentry problem [1, 7, 8], as well as a mix of PSO and GA for trajectory optimization of spacecraft. Furthermore, an artificial bee colony (ABC) was employed in several studies for a hypersonic vehicle's reentry trajectory [9].

New approaches were proposed in a paper by Graichen and Petit to solve two concerns in indirect optimal control. An auxiliary optimum control problem is generated from a specified beginning trajectory of the system in the technique described. The second way involves incorporating mixed state-input limitations into the dynamics of the optimal control problem under consideration. The approach was used to solve the problem of shuttle reentry [10]. In the identical situation, Rahimi and coworkers minimized heat rate, but the final requirements, particularly azimuth angle, were not reached appropriately [1].

In the present work, the optimal control problem is described for the case of a space vehicle and the optimization of its reentry trajectory, and three global optimization methods (ABC, GA, and GA-PSO) are utilized to determine the best profiles of the bank angle and angle of attack to minimize the heat rate without final circumstances being sacrificed. The profile of the angle of attack helps to minimize heat in the first half of the trajectory, but in the second half, both the profiles of bank angle and the angle of attack are employed to meet the final criteria. Dividing guiding profiles into two halves aids in this project's completion while also reducing heat transmission.

The following is a summary of how the present paper is put together. The best trajectory design procedure is explained in Sect. 2. First, we will go through optimum control theory and optimization techniques. The suggested division guiding mechanism is then discussed in detail. In part 3, the aerodynamic, atmospheric, and gravity models are discussed in-depth, as well as the reentry vehicle's equation of motion. The present method's findings are discussed and contrasted in Sect. 4. Finally, this paper is concluded.

2 Optimal trajectory design

The ideal design of an SRV's reentry trajectory will be discussed in this section. To begin, a unique strategy for optimizing the optimum control problem will be described. The guidance law is then separated into two different components in the second section, using an inventive way. The best combination route is then constructed using the approach described above. The suggested technique is important since it provides all of the trajectory's needs with precise limitations.

2.1 Optimal trajectory method

The following equation may be used to represent the dynamic of a system:

$$\dot{\vec{x}} = f\left(\vec{x}(t), \vec{u}(t), t\right) \quad t_0 < t < t_f \tag{1}$$

The control variable vector $\vec{u} \in R^m$ and state vector $\vec{x} \in R^n$ are used to describe the aforesaid nonlinear system. The cost function may be used to think about the best trajectory, which is based on the optimal control theory [7, 11]:

$$J = \Phi\left[\vec{x}(t_f), t_f\right] + \int_{t_0}^{t_f} L\left[\vec{x}(t), \vec{u}(t), t\right] dt \tag{2}$$

where t_f denotes the final time for this work's problem. Also, as final conditions, Φ represents the penalty function for final time states. System dynamic equations $f\left(\vec{x}, \vec{u}, t\right)$ and the integral component of the cost function $L\left(\vec{x}, \vec{u}, t\right)$ plus a co-state multiplication (Eq. 4) define the Hamiltonian function $H\left(\vec{x}, \vec{\lambda}, \vec{u}, t\right)$:

$$H\left(\vec{x}, \vec{\lambda}, \vec{u}, t\right) = L\left(\vec{x}, \vec{u}, t\right) + \vec{\lambda}^T f\left(\vec{x}, \vec{u}, t\right) \tag{3}$$

$$\vec{\lambda}^T = -\partial H / \partial \vec{x} \tag{4}$$

The optimality criterion is obtained in this way: $(\partial H/\partial \vec{u}) = 0$ [12]. Two optimality requirements based on the angle of attack $\alpha(t)$ and bank angle $\beta(t)$ are examined for the SRV problem: $(\partial H/\partial \alpha) = 0$, $(\partial H/\partial \beta) = 0$ [12, 13].

The benefits of the indirect technique, such as optimality requirements, will be addressed based on optimal control theory. Finding the best control function for a high nonlinear issue like SRV, on the other hand, is very difficult. For such challenges, a mix of direct and indirect approaches is given. Both direct and indirect techniques have benefits and drawbacks [7, 8]. As a result, the major emphasis of this research is on combining a direct approach with unique series and optimization approaches. Indirect approach benefits from optimal control theory are also taken into account. In addition, three optimization techniques are studied in this study: ABC, GA, and GA-PSO.

GA is a program that simulates a population of people. The collection of genes describes the features of the GA technique. This population is subjected to recombination and selection operations. Parts of a gene are randomly modified by mutation. Recombination of two people produces a mixture, while selection eliminates the one who performs worse than the rest. The population gets more homogenous in its optimum fitness when these operators are repeatedly applied to a group of random beginning individuals. This approach may be expressed as an optimization algorithm [14–16].

The ABC is a swarm-based algorithm that mimics the honey bee swarm's exploration activity. This exploration method, similar to GA, is capable of producing exact findings. Employees, scouts, and onlookers bees are the three categories of bees in a colony. Each variety of bees performs a certain function. When nectar quality improves, the likelihood of spectators liking the food source rises. Colony limit, size, and maximum cycle are three of the critical control factors in ABC. See references [17–22] for further details.

Considering a population randomly, like the other approaches described, is the initial stage in implementing the PSO-GA algorithm. PSO-GA items would have more in common with the creation of biological creatures based on bird swarm behaviors. The created compendium would be considered directly for the following generation, and the remainder of the population would be formed by recombination processes that mutated the developed compendiums together [23–25]. In this approach, optimum control theory will be regarded as an indirect technique, as well as the three optimization methods indicated above, in order to design a new method. For more references regarding combined methods, see [26–28]. Also, an computational efficient indirect method for trajectory optimization regarding homotopy method should be considered [29].

The bank angle and angle of attack function may be computed by combining polynomial and sine functions in a creative method. The basic function is the polynomial function, whereas the sinusoidal function is used to provide oscillatory activity. The control inputs $\alpha(t)$, $\beta(t)$ as attack and bank angles are proposed in the form of series of the following functions to create optimum controls. It should be noted the coefficients of the proposed series would be achieved by optimization methods.

$$\alpha(t) = \sum_{i=1}^{N} \tau_i (t+\kappa)^i + \eta_i \sin(\xi_i (t+\kappa)) + \gamma_i \cos(\delta_i (t+\kappa)) \tag{5}$$

$$\beta(t) = \sum_{i=0}^{M} \zeta_i (t+\kappa)^i + \upsilon_i \sin(\varepsilon_i (t+\kappa)) + \theta_i \cos(\mu_i (t+\kappa)) \tag{6}$$

where the constantsτ_i,η_i,ξ_i,γ_i, δ_i, , ζ_i, υ_i, ε_i, θ_i, μ_i and κ are estimated. Moreover, N and M are real numbers (N = 1, 2, 3, …) and (M = 1, 2, 3, …).

The SRV's aerodynamic heating may be expressed using Eqs. (7, 8), where heating is specified as a function of velocity (v), altitude (h) [10]. Equations (8) and (7) with regard to the intermediate heat rate and overload heat rate throughout the whole trajectory are considered for cost function.

$$J_{\text{over}} = \max\left[q^* \left(\sum_{i=0}^{4} m_i n^i \right) \sqrt{\rho}.(V(t))^{3.07} \right] \tag{7}$$

$$J_{\text{int}} = q^* \int_0^{T_{\text{ex}}} \left(\sum_{i=0}^{4} m_i n^i \right) \sqrt{\rho}.(V(t))^{3.07} dt \tag{8}$$

T_{ex} stands for the intermediate time. In the above equations, m and n are coefficients of polynomials. In addition, the optimizer employs the penalty function as terminal's cost regarding Eq. (9).

$$J_{\text{terminal}} = \sum_{i=1}^{5} \sigma_i \left| \left(X_i(tf) - X_i^{\text{nom}}(tf) \right) \right| \tag{9}$$

As a result, the total cost function is proposed which is written as follows:

$$J_{\text{total}} = J_{\text{over}} + J_{\text{int}} + J_{\text{terminal}} \tag{10}$$

where $X_i(T)$, $i = [1, \ldots, 5]$ are the dynamic system states for SRV, with $i = 1$ representing height,$i = 2$ representing velocity,$i = 3$ representing flight path angle,$i = 4$ representing azimuth, and $i = 5$ representing latitude. To normalize the parameters in the same order, the weight coefficients σ_i are employed.

In this study's computational approach, the optimizer first estimates the bank angle and angle of attack profiles for the SRV problem using Eqs. (5) and (6). The optimizer also calculates the co-state values at the trajectory's end. After that, by integrating the system of differential equations with regard to the given boundary conditions, the state (Eq. 1) and co-state (Eq. 4) equations are obtained. The optimality requirements ($\partial H/\partial\alpha$, $\partial H/\partial\beta$) and the cost function J_{total} are calculated at the end. Sub-criteria in the cost function include (i) maximal heat (Eq. 7), (ii) total heat throughout the trajectory (Eq. 8), and (iii) terminal requirements (Eq. 9). The optimum solution that fulfills both optimal and optimization control techniques would be found by verifying the optimality requirements. The optimizer seeks to minimize the cost function to fulfill the heat and final requirements if the convergence trends from all sections of the algorithm are acceptable (for example, the absence of singularity).

2.2 The proposed guidance

The suggested method's major purpose is to reduce the heat rate while maintaining the final conditions. The flight route is broken into two segments to accomplish this. The major emphasis of the guiding challenge in the first step was the decrease in heat rate owing to the vehicle's high speed (Mach number about 25, see ref. [10]). According to the findings of this study, the profile of the angle of attack has the greatest influence on the quantity of heat rate. This resulted from raising the maximum value of the initial altitude peak. As a result, the vehicle speed is lowered in this phase, and therefore the heat transfer rate is reduced. As a result, the cost function in the first step of the trajectory may be described by a combination of overall heat and maximal heat (Eq. 11).

$$J_{\text{phase1}} = r_1 J_{\text{over}} + r_2 J_{\text{int}} \tag{11}$$

where r_1 and r_2 are selected as 1 and 0.0001, respectively, based on the level of skill gained via this effort. From Eq. (5), the profile of the angle of attack may be defined as follows:

$$\alpha(t) = (\tau_1 t + \tau_2) + \eta_1 \sin(\xi_1 t) + \gamma_1 \cos(\delta t) \tag{12}$$

The key focus in the second step of the trajectory is the fulfillment of the final requirements and the minimizing of the following cost function:

$$J_{\text{phase2}} = J_{\text{int}} + J_{\text{terminal}} \tag{13}$$

To accomplish the objective, history determination of both angle of attack and bank angle are important. So, the bank angle and the angle of attack profiles are proposed for SRV as follows from Eqs. (5) and (6):

$$\beta(t) = (\tau_3(t+\kappa) + \tau_4) + \eta_2 \sin(\xi_2(t+\kappa)) + \gamma_2 \cos(\delta t) \tag{14}$$

$$\alpha(t) = (\tau_5(t+\kappa) + \tau_6) + \eta_3 \sin(\xi_3(t+\kappa)) + \gamma_3 \cos(\delta t) \tag{15}$$

3 Case study

The spacecraft reentry model, which includes all vehicle characteristics, control variables, a flight dynamic model, and final and initial conditions, is studied in the first portion of this section. The above strategy is used in the case study, and the simulation results are described and analyzed.

3.1 Spacecraft reentry vehicle model

A space reentry vehicle problem was chosen as the case study for trajectory optimization. The issue is very sensitive to numerical solutions, and the return mission has a longer flight duration. The space reentry vehicle's motion equations are as follows [10]:

$$\dot{h} = v \sin(\gamma) \tag{16}$$

$$\dot{v} = -\frac{D(h, v, \alpha)}{m} - g(h)\sin(\gamma) \tag{17}$$

$$\dot{\gamma} = \frac{L(h, v, \alpha)}{mv}\cos(\beta) + \cos(\gamma)\left(\frac{v}{R_e + h} - \frac{g(h)}{v}\right) \tag{18}$$

$$\dot{\theta} = \frac{v}{R_e + h}\cos(\gamma)\cos(\psi) \tag{19}$$

$$\dot{\psi} = \frac{L(h, v, \alpha)}{mv\cos\gamma}\sin(\beta) + \frac{v}{R_e + h}\cos(\gamma)\sin(\psi)\sin(\theta) \tag{20}$$

$$\dot{\phi} = \frac{v}{R_e + h}\cos(\gamma)\sin(\psi)/\cos(\theta) \tag{21}$$

The system states are altitude h, velocity v, flight path angle γ, azimuth ψ, latitude θ, and longitude ϕ. Because the bank angle $\beta(t)$ and the angle of attack $\alpha(t)$ are two control variables, the lift and drag force equations are derived as a linear function of the angle of attack [10]:

$$L(h, v, \alpha) = \frac{1}{2} C_L(\alpha) \times \rho(h) \times v^2, \quad \text{where } C_L(\alpha) = a_0 + a_1\alpha \tag{22}$$

$$D(h, v, \alpha) = \frac{1}{2} C_D(\alpha) \times \rho(h) \times v^2, \quad C_D(\alpha) = b_0 + b_1\alpha + b_2\alpha^2 \tag{23}$$

At high speeds, the aerodynamic coefficients C_D and C_L are specified as functions that solely rely on the angle of attack, and they are expected to remain almost constant as the Mach number varies. Air density and gravity in the atmospheric model are solely linked to altitude, as shown below [10]:

$$g(h) = \mu/(R_e + h)^2, \ \rho(h) = \rho_0 \exp[-h/h_r] \tag{24}$$

The corresponding parameters in the above equations are provided in Table 1.

The space reentry vehicle's initial requirements are as follows:

$$\begin{array}{ll} h(0) = 79.248(\text{Km}) & \phi(0) = 0(\text{deg}) \\ v(0) = 28,090(\text{Km/h}) & \theta(0) = 0(\text{deg}) \\ \psi(0) = 90(\text{deg})\phi & \gamma(0) = -1(\text{deg}) \end{array}$$

The spacecraft's aerodynamic heating is described as a function of velocity, attack angle, and height [10]:

$$q_r(\alpha, h, v) = q^*\left(\sum_{i=0}^{4} m_i n^i\right)\sqrt{\rho(h)} \times (V(t))^{3.07} \tag{25}$$

Table 1 Constant values

Symbol	Value	Symbol	Value	Symbol	Value
μ	398,603.2 (Km^3/s^2)	ρ_0	1.225 (Kg/m^3)	R_e	6,371.2 (Km)
h_r	7.25 (Km)	S	249.91 (m2)	m	2,861.96 (Kg)
a_0	− 0.20704	a_1	1.675557	b_0	0.07854
b_1	− 0.352896	b_2	2.039962	c_0	1.06723181
c_1	− 1.1018767	c_2	0.698787	c_3	− 0.19029629

Table 2 Parameters of the space vehicle at final time

Parameters	Values at the final time
Height(h)	24,062 (m)
Velocity(v)	751 (m/s)
Flight path angle (γ)	− 0.104 (rad)
Azimuth (ψ)	0.1471 (rad)
Latitude (θ)	0.601 (rad)

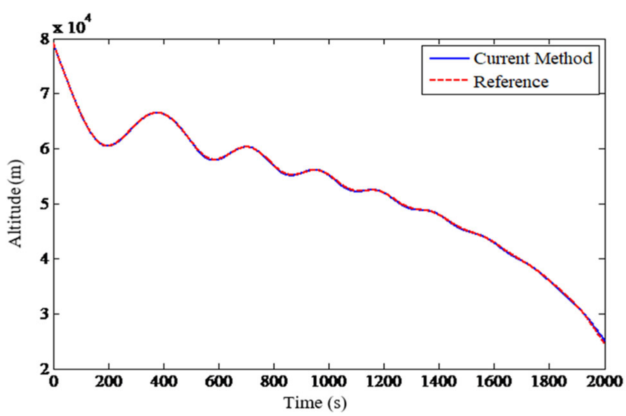

Fig. 1 Validation of state altitude with ref. [10]

where $q^* = 3.7156 \times 10^{-8}\left(\sqrt{kg/m^3}\right)$ and m_i are given in Table 1. Also, the nominal values for the states at the end of the journey are listed in Table 2.

The approach of this study was compared to reference [10] in order to verify it. The findings for all states, as can be seen, are perfectly consistent with the findings of reference [10]. As a result, the present study's flight dynamic model and optimization technique are both valid. The following are the outcomes (Figs. 1, 2, 3, 5 and 6).

In this case, the vectors $\vec{\tau}$ and $\vec{\upsilon}$ are treated as zero. M and N are three and four, respectively, and$\kappa = 0$. As a result, the suggested vectors, $\vec{\eta}$ and $\vec{\xi}$ for the angle of attack $\alpha = \alpha\left(\vec{\eta}, \vec{\xi}, \vec{\gamma},\right)$ and $\vec{\zeta}$ for the bank angle$\beta = \beta\left(\vec{\zeta}, \vec{\gamma}\right)$, are derived using the approach described in this paper:

=[17.4641, − 0.0574, 0.4738, 0.0085, − 0.0071].

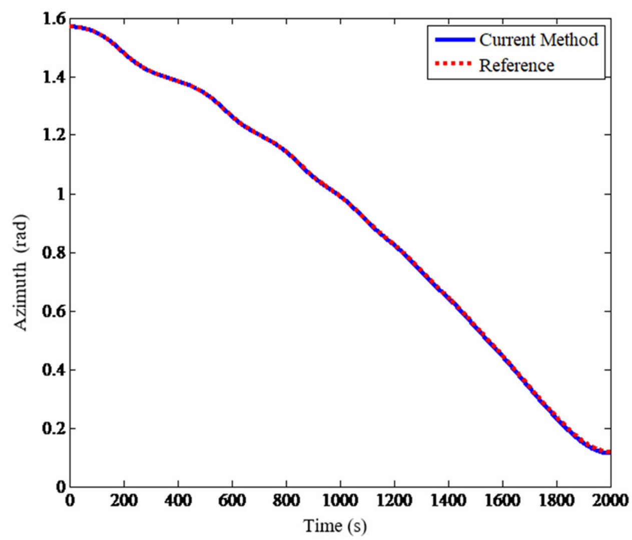

Fig. 2 Validation of state Azimuth angle with ref. [10]

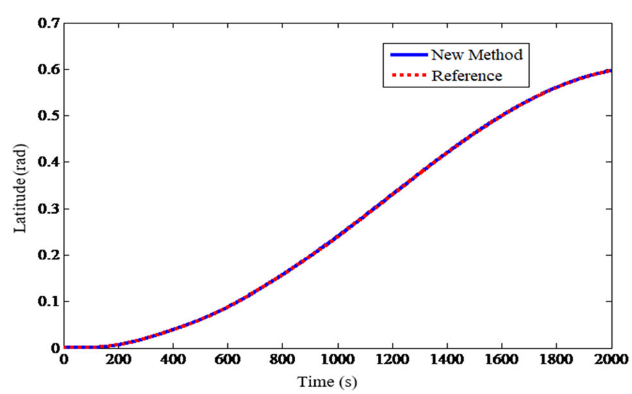

Fig. 3 Validation of state latitude angle with ref. [10]

$\vec{\xi}$=[− 0.0052, − 0.0017, 0.0036, − 0.0066].

$\vec{\zeta}$ = [− 0.002, 0.1036, 2.434, − 74.938].

$\vec{\gamma}$ = [0.034, 0.0045, 0.127, − 5.768].

3.2 Simulation results

In the dividing guidance method, the trajectory is divided into two phases as one of the novelties of this work. In

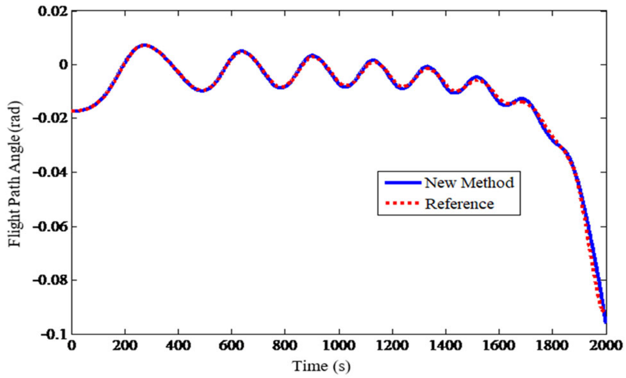

Fig. 4 Validation of state flight path angle with ref. [10]

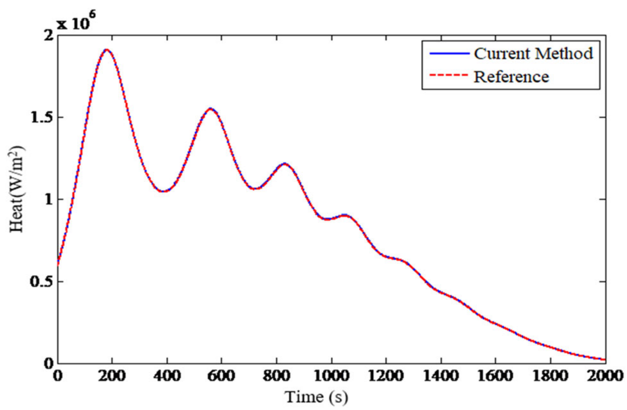

Fig. 5 Validation of heat transfer rate with ref. [10]

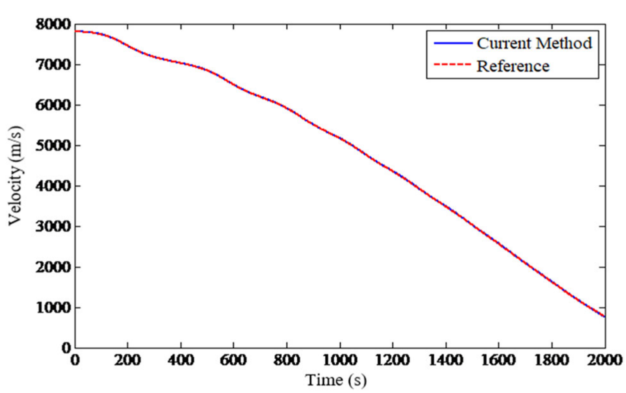

Fig. 6 Validation of state velocity with ref. [10]

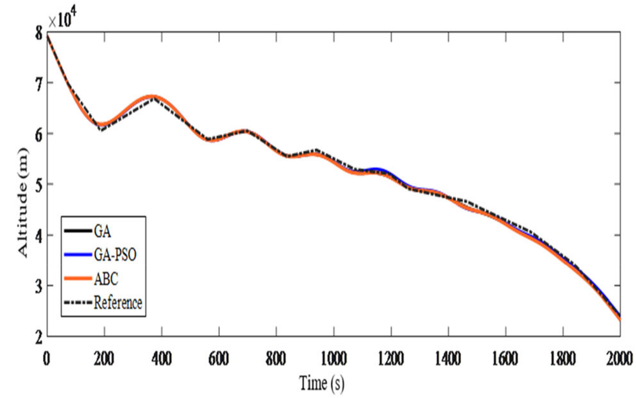

Fig. 7 Altitude–time

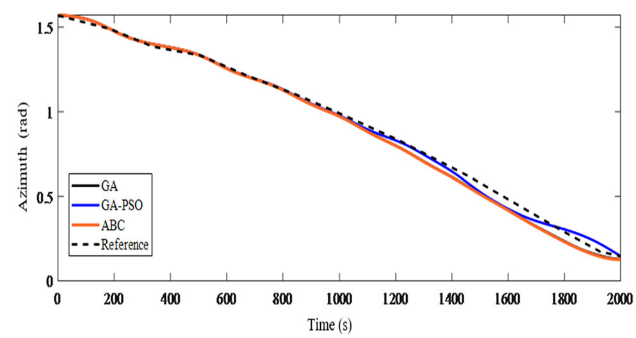

Fig. 8 Azimuth angle–time

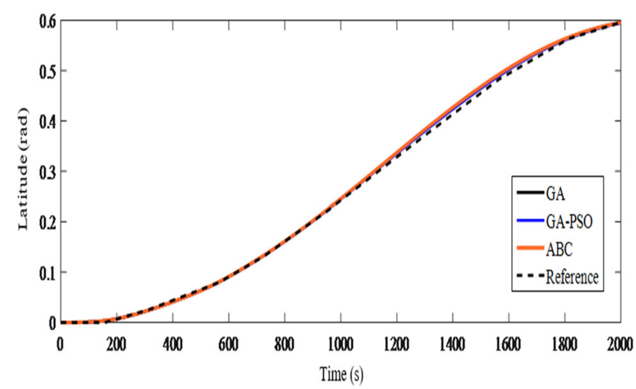

Fig. 9 Latitude angle–time

the first phase, named as “Heat Reduction,” the focus is on the minimization of heat rate by considering the effect of attack angle in cost functions. Next phase belongs to satisfy final conditions by mainly focusing on the bank angle profile. The parameter κ optimization methods, artificial bee colony (ABC) and genetic algorithm (GA), and GA-PSO. The results of each method are compared to the other methods and reference [10]. The results including time history of state variables, heat reduction, and optimality conditions are mentioned in the following figures: indicates the trajectory dividing time that in the current study, it is set to 1000 s. As shown in Figs. 7, 8, 9, 10, 11, 12 and 13, all of the chosen optimization approaches are effective in addressing the SRV optimum control problem using the suggested algorithm of this study. They are all capable of slowing down the heat rate and adjusting to the final requirements. As a result, these two commendable benefits of heat reduction and fulfilling final conditions are referred to as two-phase guidance. GA-PSO,

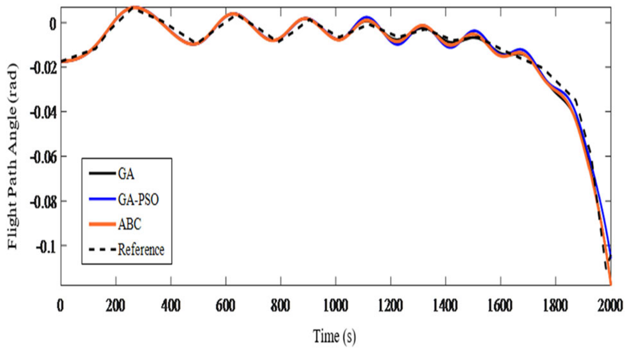

Fig. 10 Flight path angle–time

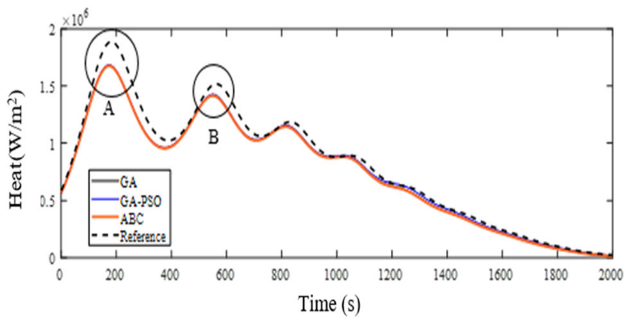

Fig. 11 Heat transfer–time

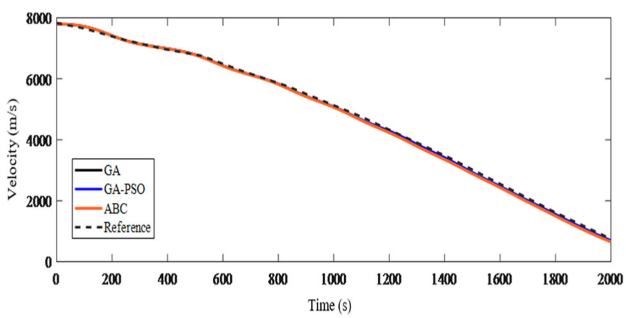

Fig. 12 Velocity–time

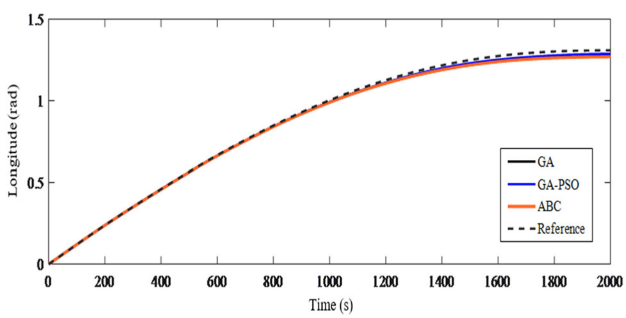

Fig. 13 Longitude–time

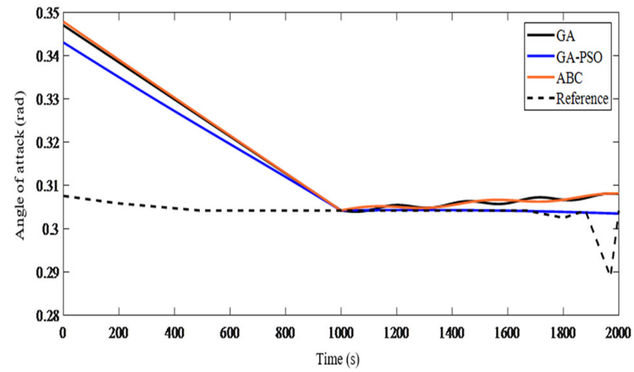

Fig. 14 Angle of attack–time

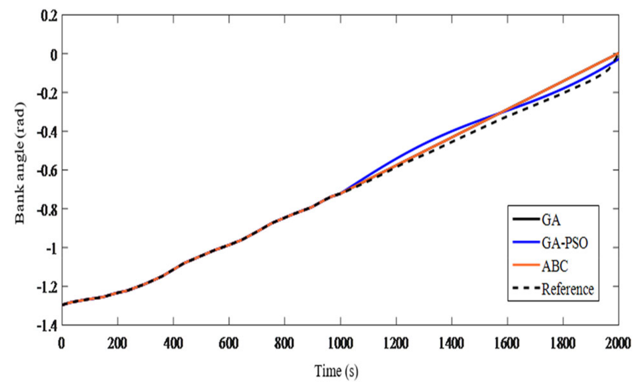

Fig. 15 Bank angle–time

on the other hand, has the greatest outcomes and the fewest faults of all.

As shown in Fig. 14, two sections, A and B, have a significant role in lowering the heat rate. Both the largest quantity of heat rate and the level below the heating plot are minimized in sections A and B. Figures 14 and 15 illustrate the profiles of the angle of attack and the bank angle for each method. Figure 16 depicts the resultant trajectory of each approach.

To provide additional understanding, the findings of each approach are shown individually in a table, and the methods are then compared in Table 6. From Tables 3, 4, 5 and 6, it is clear that the GA-PSO approach yielded the best results. Overall heat is lowered by 6% using the previously indicated method. It was critical to lower the heat in this stage of the flight since the time interval (140–250 s) is the period of ablation in the SRV's reentry phase. As a result, the overall heat in the time range of 140 to 250 s is lowered by roughly 11%, as is the maximum heat rate. The final requirements are met accurately, with the biggest mistake being about 2% for

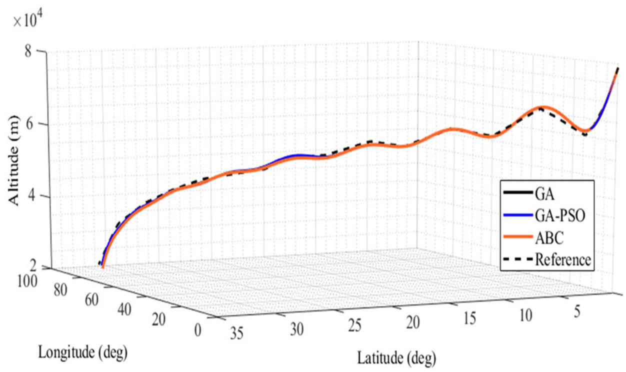

Fig. 16 Three-dimensional trajectory by three optimizers

Table 3 Comparison of GA-PSO method and the reference values

Parameter	GA-PSO	Reference [10]	Percent of difference
Overall Heat (W.s/m^2)	1.1586831e + 09	1.236611737e + 09	− 6.3%*
Overall Heat [140–250 s] (W.s/m^2)	1.7373867e + 08	1.960612781e + 08	− 10.6%
Max Heat(W/m^2)**	1.6835991e + 06	1.88791064e + 06	− 10.14%
Final Latitude [rad]	0.5949	0.5963	− 0.2%
Final Altitude [m]	24,008.7912	24,062	− 0.2%
Final Velocity [m/s]	734	751	− 2.3%
Final Flight Path Angle[rad]	− 0.1059	− 0.104	− 1.8%
Final Azimuth [rad]	0.1478	0.1471	0.4%

*Hint: The negative sign in the column of the percentage represents the percentage of the decrease

**It should be noted that maximum of heat transfer is occurred at time about 180 s

the final velocity. Overall, heat transmission is lowered by the other optimization approaches as well, but the ultimate criteria are not reached as well. For example, the azimuth inaccuracy in GA is roughly 12%, whereas the error in ABC is about 14%.

Finally, one can conclude the best result from heat reduction and satisfaction Finally, the specified algorithm (see Sect. 2.2) and the PSO-GA optimization technique obtain the best result in heat reduction and fulfillment of final requirements. The features of the PSO-GA optimizer are given in Table 7 in the current situation.

Table 4 Comparison of the ABC method and the reference values

Parameter	ABC	Reference [10]	Percent of difference
Overall heat (W s/m^2)	1.15079193e + 09	1.236611737e + 09	− 6.9%
Overall heat [140–250 s] (W s/m^2)	1.72956373e + 08	1.960612781e + 08	− 11.8%
Max heat (W/m^2)	1.67637533e + 06	1.88791064e + 06	− 11.25%
Final latitude [rad]	0.5960	0.5963	− 0.05%
Final altitude [m]	23,256	24,062	− 3.3%
Final velocity [m/s]	686	751	− 8.6%
Final flight path angle[rad]	− 0.1179	− 0.104	− 13.3%
Final azimuth [rad]	0.1269	0.1471	− 13.7%

Table 5 Comparison of the GA method and the reference values

Parameter	GA	Reference [10]	Percent of difference
Overall heat (W s/m^2)	1.1519646e + 09	1.236611737e + 09	− 6.8%
Overall heat [140–250 s] (W s/m^2)	1.7300106e + 08	1.960612781e + 08	− 11.7%
Max heat(W/m^2)	1.6760813e + 06	1.88791064e + 06	− 11.17%
Final latitude [rad]	0.5959	0.5963	− 0.062%
Final altitude [m]	23,323	24,062	− 3%
Final velocity [m/s]	691	751	− 8%
Final flight path angle [rad]	− 0.1177	− 0.104	− 13.1%
Final azimuth [rad]	0.1298	0.1471	− 11.7%

With the GA-PSO computations, the profiles parameters of bank angle and angle of attack are derived as shown in Table 8.

Figures 17 and 18 demonstrate the optimality conditions of bank angle and attack angle. Figures show that both of the optimality requirements ($(\partial H/\partial \alpha) = 0$, $(\partial H/\partial \beta) = 0$) are appropriately met owing to their values being close to zero.

Table 6 Comparison of the three optimizers with respect to reference [10]

Parameter	GA-PSO	GA	ABC
Overall heat (W s/m^2)	– 6.3%	– 6.8%	– 6.9%
Overall heat (W s/m^2) [140–250 s]	– 10.6%	– 11.7%	– 11.8%
Max heat (W/m^2)	– 10.14%	– 11.17%	– 11.25%
Final latitude [rad]	– 0.2%	– 0.062%	– 0.05%
Final altitude [m]	– 0.2%	– 3%	– 3.3%
Final velocity [m/s]	– 2.3%	– 8%	– 8.6%
Final flight path angle [rad]	– 1.8%	– 13.1%	– 13.3%
Final azimuth [rad]	0.4%	– 11.7%	– 13.7%

Table 7 Optimizer parameters

Parameters	Values
Number of optimization parameters	12
Number of generations	150
Population size	1500
Keep percent	0.3
Cross-percent	0.2
Mutation percent	0.05

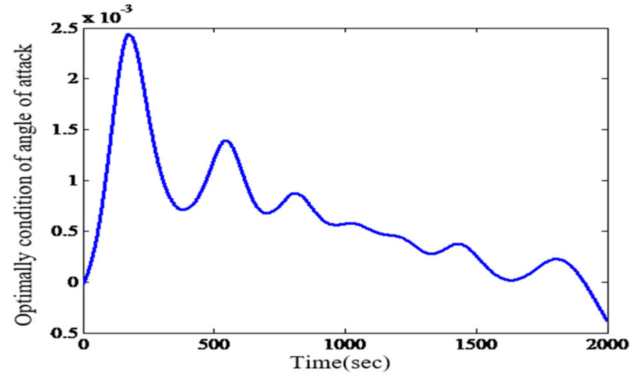

Fig. 17 Optimality condition for angle of attack for GA-PSO method

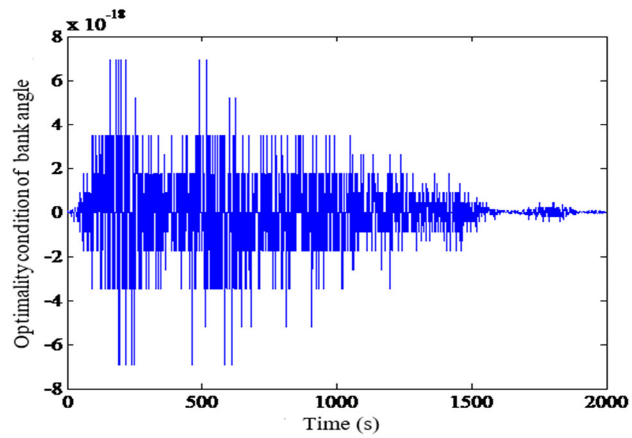

Fig. 18 Optimality condition for bank angle for GA-PSO method

4 Conclusions

Based on optimization technique and optimal control theory with regard to a unique suggested algorithm and approach, the best trajectory for a spacecraft reentry vehicle in the reentry phase is examined in this study. As a test case, the optimum control problem is defined on SRV. The optimal bank angle and angle of attack profiles are determined using three global optimization techniques (ABC, GA, and GA-PSO). The purpose of optimum trajectory design is to lower the heat rate while maintaining ideal final conditions. The current technique for achieving this aim is to divide the trajectory into two parts. Heat rate is particularly significant in the initial phase, and the heat rate value may be minimized by designing the attack angle. As a result, a time series is used to parameterize the attack angle profile. The optimizers reduced the heat rate or a combination of heat rate and final conditions by minimizing the cost function. In the first step, the cost function is the maximum heat plus the heat integral over time. Both bank angle and angle of attack profiles might be employed to meet the final criteria in the second step. The GA-PSO approach has proved to be the best and most logical in producing outcomes based on the results. The total heat is decreased by approximately 6%, and heat transmission in the [140–250 s] time period is lowered by around 11% using this strategy. Furthermore, the present approach reduces the maximum heat rate by around 12%. As a result, all of the final conditions mistakes are less than 2%. As a result, the present study's approach might be used to reduce the heat rate of an SRV without sacrificing final conditions.

Table 8 Values of the $\alpha(t)$ and $\beta(t)$ profile parameters

Parameters	Values	Parameters	Values
τ_1	– 0.0022427	η_1	13.947028
τ_2	19.656329	η_2	44.965454
τ_3	0.041389	η_3	– 25.661362
τ_4	– 41.270	ξ_1	– 5
τ_5	– 0.0000510	ξ_2	0.1091104
τ_6	17.4301	ξ_3	– 2.833096

Funding Not applicable.

Declarations

Conflict of interest The authors declare that they have no conflict of interest.

References

1. Rahimi A, Dev Kumar K, Alighanbari H (2012) Particle swarm optimization applied to spacecraft reentry trajectory. J Guid Control Dyn 36(1):307. https://doi.org/10.2514/1.56387
2. Pontryagin LS (1987) The mathematical theory of optimal processes. CRC Press
3. Betts JT, Kolmanovsky I (2002) Practical methods for optimal control using nonlinear programming. Appl Mech Rev 55:B68. https://doi.org/10.1115/1.1483351
4. Hargraves CR, Paris SW (1987) Direct trajectory optimization using nonlinear programming and collocation. J Guid Control Dyn 10(4):338. https://doi.org/10.2514/3.20223
5. Gurfil P, Kasdin NJ (2002) Niching genetic algorithms-based characterization of geocentric orbits in the 3D elliptic restricted three-body problem. Comput Methods Appl Mech Eng 191:5683–5706. https://doi.org/10.1016/S0045-7825(02)00481-4
6. Yokoyama N, Suzuki S (2005) Modified genetic algorithm for constrained trajectory optimization. J Guid Control Dyn 28(1):139. https://doi.org/10.2514/1.3042
7. Shafieenejad I, Novinzadeh AB, Molazadeh VR (2014) Comparing and analyzing min-time and min-effort criteria for free true anomaly of low-thrust orbital maneuvers with new optimal control algorithm. Aerosp Sci Technol 4(35):116–134. https://doi.org/10.1016/j.ast.2014.03.009
8. Shafieenejad I, Novinzadeh AB, Molazadeh VR (2015) Introducing a novel algorithm for minimum-time low-thrust orbital transfers with free initial condition. Proc Inst Mech Eng G J Aerosp Eng 229(2):333–351. https://doi.org/10.1177/0954410014533311
9. Duan H, Li S (2015) Artificial bee colony–based direct collocation for reentry trajectory optimization of hypersonic vehicle. IEEE Trans Aerosp Electron Syst 51(1):615–626. https://doi.org/10.1109/TAES.2014.120654
10. Graichen K, Petit N (2008) Constructive methods for initialization and handling mixed state-input constraints in optimal control. J Guid Control Dyn 31(5):1334–1343. https://doi.org/10.2514/1.33870
11. Berend N, Talbot C (2006) Overview of some optimal control methods adapted to expendable and reusable launch vehicle trajectories. Aerosp Sci Technol 10(3):222–232. https://doi.org/10.1016/j.ast.2005.11.004
12. Peng H, Yang C, Li Y, Zhang S, Chen B (2013) Surrogate-based parameter optimization and optimal control for optimal trajectory of Halo orbit rendezvous. Aerosp Sci Technol 26(1):176–184. https://doi.org/10.1016/j.ast.2012.04.001
13. Pan B, Lu P, Pan X, Ma Y (2016) Double-homotopy method for solving optimal control problems. J Guid Control Dyn doi 10(2514/1):G001553
14. Davis L (1991) Handbook of genetic algorithms. Van Nostrand Reinhold, New York
15. Gen M, Cheng R (2000) Genetic algorithms and engineering optimization, vol 7. Wiley, Newyork
16. Srinivas M, Patnaik LM (1994) Genetic algorithms: a survey. Computer 27(6):17–26. https://doi.org/10.1109/2.294849
17. Karaboga D, Basturk B (2007) A powerful and efficient algorithm for numerical function optimization: artificial bee colony (ABC) algorithm. J Glob Optim 39(3):459–471. https://doi.org/10.1007/s10898-007-9149-x
18. Karaboga D, Basturk B (2008) On the performance of artificial bee colony (ABC) algorithm. Appl Soft Comput 8(1):687. https://doi.org/10.1016/j.asoc.2007.05.007
19. Karaboga D, Akay B (2009) A comparative study of artificial bee colony algorithm. Appl Math Comput 214(1):108–132. https://doi.org/10.1016/j.jfranklin.2008.11.003
20. Akay B, Karaboga D (2012) Artificial bee colony algorithm for large-scale problems and engineering design optimization. J Intell Manuf 23(4):1001–1014. https://doi.org/10.1007/s10845-010-0393-4
21. Yusup N, Sarkheyli A, Zain AM, Hashim SZM, Ithnin N (2014) Estimation of optimal machining control parameters using artificial bee colony. J Intell Manuf 25(6):1463. https://doi.org/10.1007/s10845-013-0753-y
22. Ramadan HS, Fathy A, Becherif M (2017) Optimal gain scheduling of VSC-HVDC system sliding mode control via artificial bee colony and mine blast algorithms. IET Gener Trans Distrib 12(3):661. https://doi.org/10.1049/iet-gtd.2017.0935
23. Samani M, Tafreshi M, Shafieenejad I, Nikkhah AA (2015) Minimum-time open-loop and closed-loop optimal guidance with GA-PSO and neural-fuzzy for Samarai MAV flight. IEEE Aerosp Electron Syst Mag 30:28–37. https://doi.org/10.1109/MAES.2015.7119822
24. Chen W, Panahi M, Pourghasemi HR (2017) Performance evaluation of GIS-based new ensemble data mining techniques of adaptive neuro-fuzzy inference system (ANFIS) with genetic algorithm (GA), differential evolution (DE), and particle swarm optimization (PSO) fo landslide spatial modelling. CATENA 157:310–324. https://doi.org/10.1016/j.catena.2017.05.034
25. Abdulkhader HK, Jacob J, Mathew AT (2018) Fractional-order lead-lag compensator-based multi-band power system stabiliser design using a hybrid dynamic GA-PSO algorithm. IET Gener Transm Distrib 12:3248–3260. https://doi.org/10.1049/iet-gtd.2017.1087
26. Liu Y, Li X et al (2022) Evolutionary multi-objective trajectory optimization for a redundant robot in Cartesian space considering obstacle avoidance. Mech Sci 13:41–53. https://doi.org/10.5194/ms-13-41-2022
27. Zhang S (2022) An optimal design scheme of missile trajectory. journal of physics: conference series. In: 2022 International conference on automation and space science & technology. https://doi.org/10.1088/1742-6596/2220/1/012012
28. Ta E, Ar V, John L (2021) Costate mapping for indirect trajectory optimization. Astrodynamics 5:359–371. https://doi.org/10.1007/s42064-021-0114-0
29. Yang H, Li S, Bai X (2019) Fast homotopy method for asteroid landing trajectory optimization using approximate initial costates. J Guid Control Dyn 42(3):585–597. https://doi.org/10.2514/1.G003414